The EMBO Journal Vol. 20 No. 10 pp. 2349–2356, 2001

Suppression of inflammatory and neuropathic pain symptoms in mice lacking the N-type Ca^{2+} channel

Hironao Saegusa, Takashi Kurihara, Shuqin Zong, An-a Kazuno, Yoshihiro Matsuda, Takahiro Nonaka, Wenhua Han, Hideyuki Toriyama and Tsutomu Tanabe[1]

Department of Pharmacology and Neurobiology, Graduate School of Medicine, Tokyo Medical and Dental University and CREST, Japan Science and Technology Corporation, 1-5-45 Yushima, Bunkyo-ku, Tokyo 113-8519, Japan

[1]Corresponding author
e-mail: t-tanabe.mphm@tmd.ac.jp

H.Saegusa and T.Kurihara contributed equally to this work

The importance of voltage-dependent Ca^{2+} channels (VDCCs) in pain transmission has been noticed gradually, as several VDCC blockers have been shown to be effective in inhibiting this process. In particular, the N-type VDCC has attracted attention, because inhibitors of this channel are effective in various aspects of pain-related phenomena. To understand the genuine contribution of the N-type VDCC to the pain transmission system, we generated mice deficient in this channel by gene targeting. We report here that mice lacking N-type VDCCs show suppressed responses to a painful stimulus that induces inflammation and show markedly reduced symptoms of neuropathic pain, which is caused by nerve injury and is known to be difficult to treat by currently available therapeutic methods. This finding clearly demonstrates that the N-type VDCC is essential for development of neuropathic pain and, therefore, controlling the activity of this channel can be of great importance for the management of neuropathic pain.

Keywords: $Ca_v2.2$/gene targeting/N-type calcium channel/pain

Introduction

The voltage-dependent Ca^{2+} channel (VDCC) is a molecular complex containing several subunits named α_1, α_2–δ, β and γ (Catterall, 1998; Hofmann *et al*., 1999). The α_1-subunit is essential for channel functions and determines fundamental channel properties. VDCCs are classified into several groups (L-, N-, P-, Q-, R- and T- types) based on electrophysiological and pharmacological properties. On the other hand, molecular biological studies have identified 10 different cDNAs each coding for an α_1-subunit in various tissues of mammalian species and they are divided into three groups (Ca_v1, Ca_v2 and Ca_v3 families) according to their sequence similarities (Ertel *et al*., 2000). The Ca_v1 family ($Ca_v1.1$, 1.2, 1.3 and 1.4, also referred to as α_{1S}, α_{1C}, α_{1D} and α_{1F}, respectively) corresponds to dihydropyridine-sensitive L-type channels, and the Ca_v3 family ($Ca_v3.1$, 3.2 and 3.3, also referred to as α_{1G}, α_{1H} and α_{1I}, respectively) corresponds to low-voltage activated T-type channels. Neuronal high-voltage activated channels resistant to dihydropyridines contain an α_1-subunit belonging to the Ca_v2 family, which includes $Ca_v2.1$, $Ca_v2.2$ and $Ca_v2.3$ (also referred to as α_{1A}, α_{1B} and α_{1E}, respectively). $Ca_v2.1$ is thought to support the P- and Q-type Ca^{2+} currents and to play critical roles in neurotransmitter release at central synapses. $Ca_v2.3$ is thought to contribute to the R-type channel first identified in cerebellar granule cells (Zhang *et al*., 1993; Piedras-Renteria and Tsien, 1998; Tottene *et al*., 2000), though controversy still exists as to whether this subunit also constitutes the T-type channel. With regard to $Ca_v2.2$, protein purification studies have shown that this subunit is a component of the N-type channel (Witcher *et al*., 1993), which, like P/Q-type channels, plays critical roles in the regulation of neurotransmitter release (Catterall, 1998).

Recently, mice with a targeted mutation in each of the $Ca_v2.1$ and $Ca_v2.3$ channels have been reported. $Ca_v2.1$-null mice showed progressive ataxia and absence epilepsy, and the important roles of $Ca_v2.1$ channels in synaptic transmission were demonstrated (Jun *et al*., 1999). $Ca_v2.3$-null mice showed increased anxiety and abnormal nociceptive and antinociceptive behaviors, suggesting multiple roles for the $Ca_v2.3$ channel in the nervous system (Saegusa *et al*., 2000). Thus, studies with mice carrying a null mutation for the Ca^{2+} channel can provide valuable information on the physiological functions of the channel, and therefore mice mutant for the $Ca_v2.2$ channel have been awaited to complete the genetic analyses of the functions of the Ca_v2 family.

Recent studies have suggested that VDCCs are involved in pain transmission (Vanegas and Schaible, 2000). In particular, the N-type VDCC is thought to be important for various aspects of pain-related phenomena and, from a therapeutic point of view, its blockers such as ω-conopeptides have attracted attention as antinociceptives (Chaplan *et al*., 1994b; Malmberg and Yaksh, 1994; Bowersox *et al*., 1996; Neugebauer *et al*., 1996; Diaz and Dickenson, 1997; Sluka, 1998). It is therefore important to elucidate the contribution of the N-type VDCC to development of pain symptoms in order to understand the molecular mechanisms of pain transmission and establish novel therapeutic means.

In the present study, we have established a mouse line lacking the N-type VDCC by gene targeting and found that the mutant mice exhibited various abnormal pain-related behaviors. In particular, the homozygous mutant mice developed a markedly reduced level of neuropathic pain, which is caused by nerve injury and for which no conventional remedies have been successful (Devor and Seltzer, 1999; Woolf and Mannion, 1999). Thus, the

N-type VDCC mutant mice would provide an excellent opportunity to delineate the signal transduction mechanisms leading to neuropathic pain.

Results

Generation of $Ca_v2.2$ mutant mice

We constructed a replacement-type targeting vector, BIIIZneoII, and introduced linearized BIIIZneoII into J1 embryonic stem (ES) cells by electroporation (Figure 1A). After screening 134 G418-resistant clones, one targeted clone, which yielded germline chimeric mice, was obtained. Germline transmission of the targeted allele was confirmed by Southern blot analysis (Figure 1B). Heterozygous mutant ($Ca_v2.2$+/–) mice were intercrossed to obtain homozygous mutant ($Ca_v2.2$–/–) mice; however, ~30% of the $Ca_v2.2$–/– mice were lost before weaning (+/+:+/–:–/– = 49:97:36 at weaning). At present, the reason for the premature death of $Ca_v2.2$–/– mice is not clear. Homozygous mutant mice that survived thereafter look normal without showing any apparent motor dysfunction. To confirm the gene disruption, we have performed RT–PCR, northern blot and immunoblot analyses. All of the results indicate that the *Cacna1b* gene encoding the $\alpha_1$2.2 subunit (for nomenclature see Ertel *et al.*, 2000) is disrupted as expected (Figure 1C–E). Thus, we conclude that a null allele for *Cacna1b* was successfully produced by our targeting strategy.

To examine whether the disruption of the *Cacna1b* gene resulted in the complete loss of the N-type Ca^{2+} current, we performed electrophysiological studies. By whole-cell patch–clamp recording, Ca^{2+} currents from acutely dissociated small dorsal root ganglion (DRG) neurons were examined in both wild-type ($Ca_v2.2$+/+) and $Ca_v2.2$–/– mice. In our experimental conditions, Ba^{2+} was used as a charge carrier. First, we characterized the voltage dependence of current activation. Figure 2A shows typical superimposed current traces and averaged current–voltage (I–V) relationships in $Ca_v2.2$+/+ and $Ca_v2.2$–/– neurons. The I–V relationships were similar in both genotypes, though the I–V curve in $Ca_v2.2$–/– mice shifted slightly toward the hyperpolarizing direction.

Next we examined the effects of sequential application of VDCC blockers on the peak current evoked by voltage steps to –10 mV delivered at 10–20 s intervals. In our experiments, the DRG neurons were separated into two groups according to the cell capacitance (those <15 pF and those within the range of 18.2–38 pF). The sensitivities to toxins were essentially the same between these two groups, consistent with the previous data for rat DRG neurons (Scroggs and Fox, 1992). We therefore combined data from both groups of DRG neurons. In Figure 2B, representative time course data from $Ca_v2.2$+/+ and $Ca_v2.2$–/– DRG neurons are shown. In the $Ca_v2.2$+/+ neuron, bath application of 1 μM ω-conotoxin GVIA, an N-type channel blocker, clearly inhibited the peak Ba^{2+} current, and subsequent application of 0.2 μM ω-agatoxin IVA, a P/Q-type channel blocker, further blocked the Ba^{2+} current (Figure 2B, top). On average, ω-conotoxin GVIA blocked 30.0 ± 6.80% (n = 7) of the peak current, and subsequent application of ω-agatoxin IVA blocked 28.8 ± 2.65% (n = 5) of the original peak current in $Ca_v2.2$+/+ DRG neurons. In contrast, the same dosage of

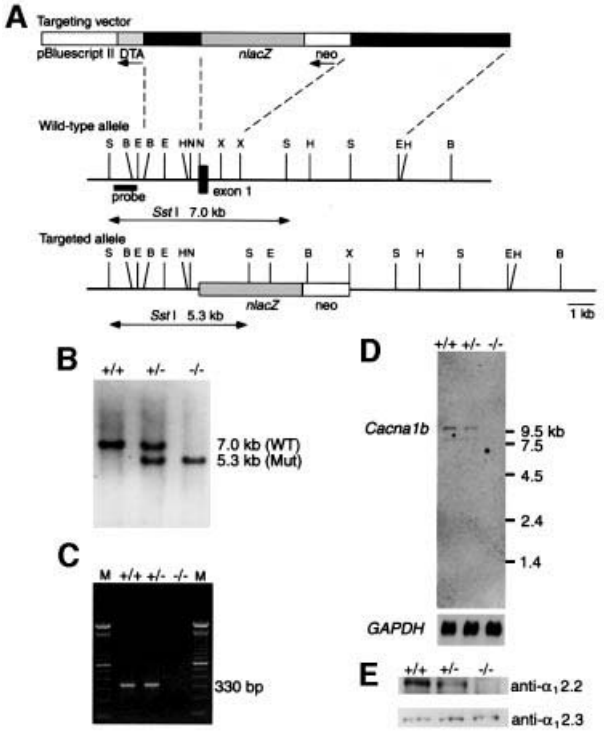

Fig. 1. Generation of mice lacking the $\alpha_1$2.2 subunit of the N-type VDCC. (**A**) A simplified restriction map around exon 1 of the *Cacna1b* gene and structure of the targeting vector. The coding region of exon 1 is boxed. neo, PGK-neo cassette; DT-A, diphtheria toxin A fragment gene; B, *Bgl*II; E, *Eco*RI; H, *Hin*dIII; N, *Not*I; S, *Sst*I; X, *Xba*I. (**B**) Southern blot analysis of tail DNA. DNA was digested with *Sst*I and the blot was hybridized with a probe shown in (A). The 7.0 kb band is derived from the wild-type allele (WT), and the 5.3 kb band from the targeted allele (Mut). (**C**) RT–PCR analysis. cDNA derived from brain total RNA was used as a template. A fragment of 330 bp is diagnostic of normal *Cacna1b* expression. M, 100 bp ladder (Gibco-BRL). (**D**) Northern blot analysis. Poly(A)$^+$ RNA (4 μg) from mouse brains was loaded in each lane. The blot was probed with a *Cacna1b* cDNA fragment (~0.7 kb) corresponding to the cytoplasmic loop between repeats II and III of $\alpha_1$2.2. A *GAPDH* probe was used as loading control (Sabath *et al.*, 1990). (**E**) Immunoblot analysis. Membrane proteins (100 μg/lane) from mouse hippocampi were probed with a rabbit polyclonal anti-$\alpha_1$2.2 (α_{1B}) (upper) or anti-$\alpha_1$2.3 (α_{1E}) antibody (lower). No $\alpha_1$2.2 protein is detected in $Ca_v2.2$–/– mice. On the other hand, $\alpha_1$2.3 protein is expressed at a similar level in all three genotypes. +/+, wild-type; +/–, heterozygote; –/–, homozygous mutant.

ω-conotoxin GVIA was almost completely ineffective and the effect was indistinguishable from the current run-down in the $Ca_v2.2$–/– DRG neurons (Figure 2B, bottom). However, subsequent application of ω-agatoxin VIA blocked the Ba^{2+} current. On average, in $Ca_v2.2$–/– DRG neurons, ω-conotoxin GVIA blocked –1.54 ± 2.65% (n = 8), and subsequent application of ω-agatoxin IVA blocked 35.8 ± 7.98% of the peak Ba^{2+} current (n = 8; not significantly different from the value obtained for $Ca_v2.2$+/+ DRG neurons), suggesting no compensatory up-regulation of P/Q-type channels in these small DRG neurons. Thus, the ω-conotoxin-sensitive N-type current is thought to be derived solely from the $Ca_v2.2$ channel.

Abnormal anxiety-related behaviors of $Ca_v2.2$ mutant mice

Although the general behaviors of the $Ca_v2.2$–/– mice, which survived to adulthood, looked normal, we

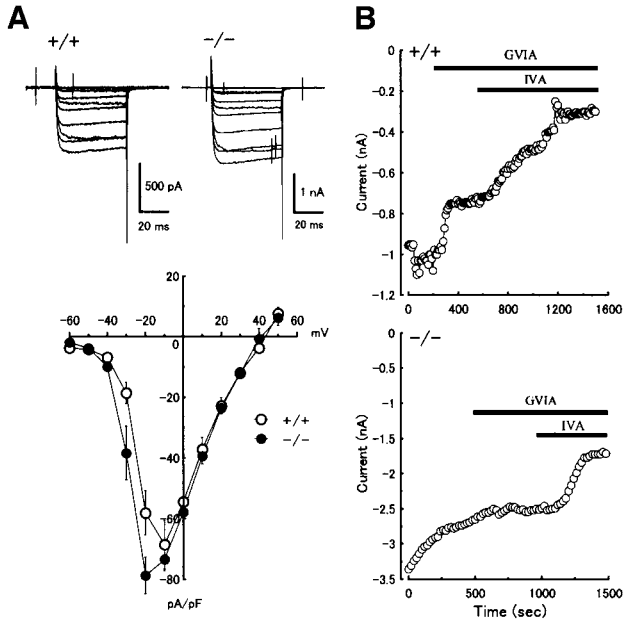

Fig. 2. Ba^{2+} currents in DRG neurons from $Ca_v2.2+/+$ and $Ca_v2.2-/-$ mice and effects of toxins on the Ba^{2+} currents. (**A**) Current–voltage relationships in $Ca_v2.2+/+$ and $Ca_v2.2-/-$ DRG neurons. Representative current traces of DRG neurons from $Ca_v2.2+/+$ (top left) and $Ca_v2.2-/-$ (top right) mice are shown. Current–voltage relationships in both genotypes of DRG neurons are shown in the bottom panel. Open circle, $Ca_v2.2+/+$; closed circle, $Ca_v2.2-/-$ (n = 4–7). Currents were elicited by a series of voltage steps from –60 to +50 mV (with 10 mV increments) delivered at 10 s intervals with holding potential at –70 mV. (**B**) Time course of inhibition of the peak Ba^{2+} currents by 1 μM ω-conotoxin GVIA (GVIA) and 0.2 μM ω-agatoxin IVA (IVA) in $Ca_v2.2+/+$ (top) and $Ca_v2.2-/-$ (bottom) DRG neurons. Peak Ba^{2+} currents, activated by 50 ms depolarization from –70 mV to –10 mV every 10 or 20 s, were plotted against time. Note that the effect of ω-conotoxin GVIA is indistinguishable from the current run-down in $Ca_v2.2-/-$ DRG neurons.

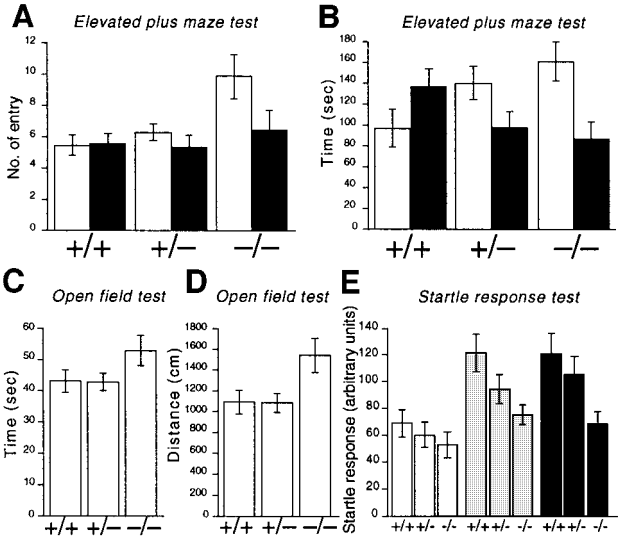

Fig. 3. Anxiety-related behaviors of wild-type (+/+), heterozygote (+/–) and homozygous mutant mice (–/–). (A and B) Elevated plus-maze test for a total of 5 min. The number of entries into each arm (**A**) and total time spent in each arm (**B**) are summarized for each genotype. Open columns: open arms; filled columns: closed arms. Entries into open arms are significantly increased in homozygous mutant mice compared with wild-type (P <0.01) and heterozygous mutant mice (P <0.05). +/+, n = 20; +/–, n = 22; –/–, n = 7. (C and D) An open-field test for a total of 2.5 min. Total locomotion time (**C**) and total path length (**D**) are summarized for each genotype. Homozygous mutant mice show significantly increased path length compared with heterozygous mutant mice (P <0.05). +/+, n = 20; +/–, n = 22; –/–, n = 9. (**E**) Startle responses to various intensities of sound pulses. Stimuli of 105 dB (open columns), 115 dB (gray columns) and 120 dB (filled columns) were given. Homozygous mutant mice show significantly decreased responses to sound stimuli of 115 and 120 dB compared with wild-type mice (P <0.05 for both sound stimuli). +/+, n = 11; +/–, n = 10; –/–, n = 7.

performed several behavioral tests to search for possible abnormalities. Each mouse was subjected to elevated plus-maze, open-field and startle response tests in this order, with an ~1 week interval between each test. In the elevated plus-maze test, we recorded the number of entries into each of the open and closed arms and time spent in each of the arms, by which the level of anxiety of the animal was assessed. Usually mice do not like to be exposed in the open arm, and $Ca_v2.2+/+$ mice actually tended to enter the closed arms preferentially and spent more time in the closed arms. However, on the contrary, $Ca_v2.2-/-$ mice entered the open arms significantly more frequently and the total time spent in the open arms in the $Ca_v2.2-/-$ mice tended to be longer (Figure 3A and B). These results suggest the lowered level of anxiety in $Ca_v2.2-/-$ mice.

We then examined the spontaneous locomotor activity and anxiety to a novel environment of the $Ca_v2.2$ mutant mice by the open-field test. The total time of movement and the total distance traveled were calculated during 2.5 min of free activity. It is thought that less activity is a sign of anxiety. The total time of behavior was not significantly different among the three genotypes (Figure 3C). However, the total distance traveled by $Ca_v2.2-/-$ mice was significantly longer (Figure 3D). This could also be a manifestation of reduced anxiety in $Ca_v2.2-/-$ mice.

Finally, we examined the acoustic startle responses of the $Ca_v2.2-/-$ mice. Mice received acoustic stimuli of 105, 115 and 120 dB in a randomized order and the startle response to each sound stimulus was recorded with an accelerometer to monitor their movement. As shown in Figure 3E, responses of $Ca_v2.2-/-$ mice are generally lower than those of $Ca_v2.2+/+$ and +/– mice. At the sound intensities of 115 and 120 dB, the responses are significantly lower in $Ca_v2.2-/-$ mice. This phenotype also seems to be compatible with the above-mentioned reduced anxiety in $Ca_v2.2-/-$ mice.

Abnormal pain responses in $Ca_v2.2$ mutant mice

As mentioned above, $Ca_v2.2$ mutant mice showed no signs of motor dysfunction. This suggests that it is possible to study pain responses of the mutant mice by assessing their behaviors towards painful stimuli. Thus we used the mutant mice to examine the contribution of the N-type VDCC to pain transmission *in vivo*.

First, responses to acute mechanical and thermal stimuli were examined. The threshold for mechanical stimuli evaluated with von Frey filaments (Chaplan *et al*., 1994a) was almost the same among $Ca_v2.2+/+$, +/– and –/– mice (Figure 4A). We also measured the threshold for noxious mechanical stimuli by the tail pressure test. Again, no significant differences were observed among the three

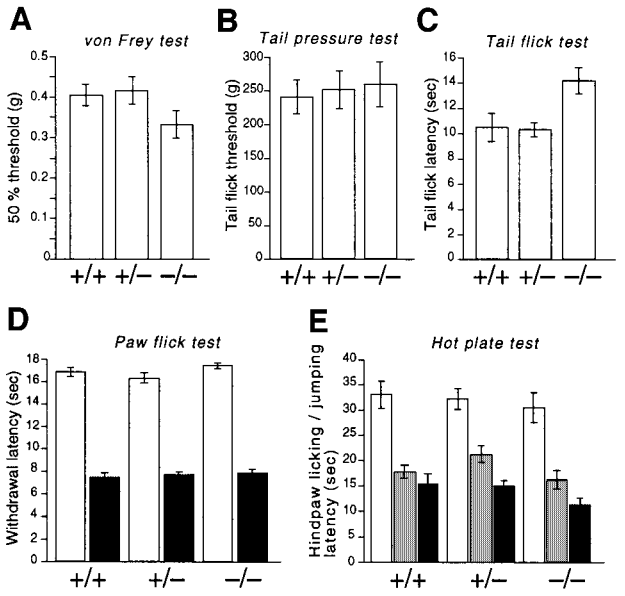

Fig. 4. Acute nociceptive responses of wild-type (+/+), heterozygote (+/–) and homozygous mutant mice (–/–). (**A**) Fifty percent hindpaw withdrawal thresholds to stimulation with von Frey hairs (+/+, n = 21; +/–, n = 29; –/–, n = 15). (**B**) Tail flick thresholds to noxious mechanical stimuli (+/+: n = 9; +/–, n = 15; –/–, n = 11). (**C**) Tail flick latencies to noxious heat (48–49°C: +/+, n = 22; +/–, n = 31; –/–, n = 17). Homozygous mutant mice show significantly prolonged latency compared with wild-type (P <0.05) and heterozygous mutant mice (P <0.01). (**D**) Hindpaw withdrawal latencies to noxious thermal stimuli with a low (infrared intensity 10, open columns) and high intensity (infrared intensity 40, filled columns). +/+, n = 21; +/–, n = 29; –/–, n = 15. (**E**) Hindpaw licking and/or jumping latencies in the hot plate tests (+/+, n = 21; +/–, n = 29; –/–, n = 15) at 50°C (open columns), 52°C (gray columns) and 55°C (filled columns).

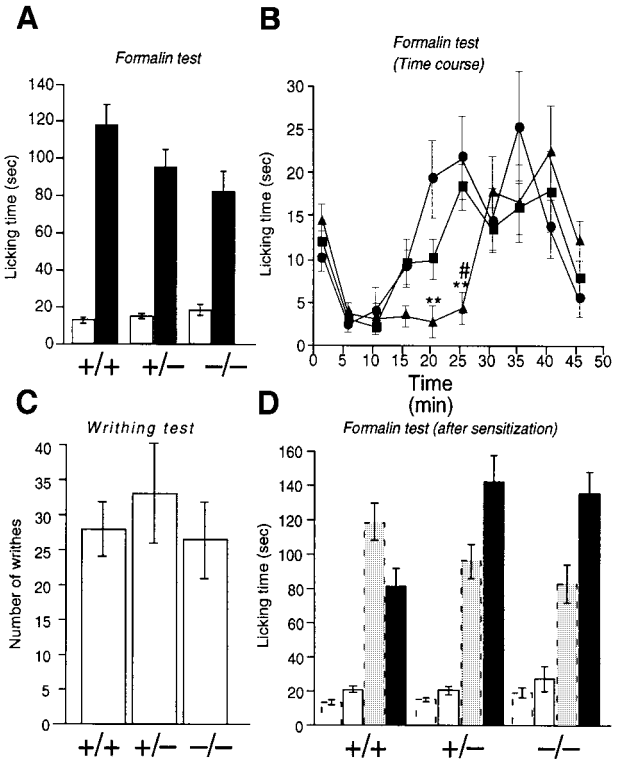

Fig. 5. Nociceptive responses to noxious chemical stimulation of cutaneous or visceral tissue. (A and B) Formalin-evoked hindpaw licking behavior. (**A**) Open columns represent total time for licking and/or biting in phase 1 (1–7 min after injection); filled columns, total licking and/or biting time in phase 2 (10–47 min after injection). +/+, n = 20; +/–, n = 27; –/–, n = 14. (**B**) The licking and/or biting time is plotted against the time after formalin injection. Circles, wild-type; squares, heterozygote; triangles, homozygous mutant. Responses in the early half of phase 2 (phase 2A, 10–27 min after injection) were almost completely suppressed in the homozygous mutant. ** represents a significant difference at P <0.01 between +/+ and –/–, and # represents a significant difference at P <0.05 between +/– and –/– at each time point. (**C**) Visceral nociceptive response (abdominal writhes) produced by intraperitoneal injection of 0.6% acetic acid (+/+, n = 8; +/–, n = 5; –/–, n = 6). (**D**) Effects of sensitization by a noxious visceral conditioning stimulus on the formalin-evoked somatic nociception. In wild-type mice, which had received a noxious visceral stimulus (0.6% acetic acid injection) 3 weeks before, the phase 2 response (filled column) was considerably reduced compared with the control (gray column). The phase 2 response in homozygous mutant mice after sensitization was significantly (P <0.05) facilitated compared with that of naive homozygous mutants. +/+, n = 6; +/–, n = 4; –/–, n = 6. Data of naive mice (columns with broken lines) are presented for comparison.

genotypes (Figure 4B). Next, we examined the responses to noxious thermal stimuli by paw flick, tail flick and hot plate tests. The paw flick and tail flick tests were used to examine the spinal reflexes at the lumbar and sacral levels, respectively, and the hot plate test examined a supraspinal involvement in nociception (Chapman *et al.*, 1985). Although $Ca_v2.2$–/– mice showed no significant differences in the response for the paw flick and hot plate tests, they showed somewhat prolonged latency in the tail flick test compared with $Ca_v2.2$+/+ and +/– mice (Figure 4C–E).

We then analyzed the responses to chemical stimuli by the formalin test and acetic acid writhing test. Injection of formalin into a mouse hindpaw elicits a biphasic pain response. In phase 1, formalin directly stimulates nociceptors to induce the pain response, and in phase 2 subsequently induced inflammation elicits the pain response (Tjølsen and Hole, 1997). The phase 1 responses of $Ca_v2.2$–/– mice, as measured by the licking/biting time, were essentially the same as those of $Ca_v2.2$+/+ and +/– mice (Figure 5A). Furthermore, the phase 2 responses of the $Ca_v2.2$–/– mice did not differ significantly from those of $Ca_v2.2$+/+ and +/– mice, although $Ca_v2.2$–/– mice tended to respond less markedly. Interestingly, however, a clear-cut statistically significant difference was observed when the time course of the response was analyzed in more detail, i.e. $Ca_v2.2$–/– mice showed significantly reduced responses in the early half of phase 2 (Figure 5B).

To determine whether the magnitude of the inflammation itself decreased, we measured the paw volume before and after administration of formalin. The magnitude of inflammation 1 h after the formalin injection, as expressed by percentage inflammation $[(V_{post} - V_{pre})/V_{pre} \times 100$, where V_{pre} and V_{post} are the paw volumes measured before and after formalin injection, respectively], was not significantly different among the three genotypes (55.6 ± 7.1% for +/+, n = 4; 66.0 ± 6.0% for +/–, n = 4; 55.8 ± 11.2% for –/–, n = 4). Therefore, the reduced pain responses in $Ca_v2.2$–/– mice do not seem to be attributable to the reduced inflammation.

We then performed the acetic acid writhing test. Intraperitoneal injection of acetic acid induces a typical behavior (writhing) in mice, which is used for quantifying

visceral pain with inflammation (Tjølsen and Hole, 1997). The number of writhes of the $Ca_v2.2$–/– mice was not significantly different from those of $Ca_v2.2$+/+ and +/– mice (Figure 5C). Recently we have established a behavioral paradigm to assess an extremely long-lasting descending antinociceptive mechanism (Kurihara *et al*., 2000). We have used this paradigm to find that $Ca_v2.3$ (α_{1E}) channel-null mutant mice have a deficit in the antinociceptive pathway (Saegusa *et al*., 2000). We also applied this test to the $Ca_v2.2$–/– mice. First, mice received an i.p. injection of acetic acid to activate the antinociceptive pathway. Three weeks later, they were subjected to the formalin test. As shown in Figure 5D, phase 1 responses were almost the same as control responses in all the genotypes. In addition, in the wild-type, phase 2 responses in the sensitized mice became weaker compared with those of naive mice when tested with formalin [a behavioral manifestation of the activated antinociceptive pathway (Kurihara *et al*., 2000)]. However, phase 2 responses in sensitized $Ca_v2.2$–/– mice increased compared with those of naive $Ca_v2.2$–/– mice (Figure 5D). Although data scattered substantially, responses in the early half of phase 2 still tended to be suppressed, whereas responses in the later half of phase 2 dramatically increased in the $Ca_v2.2$–/– mice (data not shown).

We previously reported that the $Ca_v2.3$ channel might be involved in the descending antinociceptive mechanism which is thought to contain a serotonergic system (Saegusa *et al*., 2000). Therefore we also examined the expression of *Cacna1b* in the periaqueductal gray (PAG) and rostral ventromedial medulla (RVM), both of which are suggested to be involved in the antinociceptive mechanism. Expression of *Cacna1b* was detected in a wider area of PAG than that of *Cacna1e* and was detected in the RVM including nucleus raphe magnus, where serotonergic neurons that might be involved in the pain modulatory system originate and where *Cacna1e* expression is hardly observed (not shown).

Next we studied the responses related to neuropathic pain in the $Ca_v2.2$–/– mice. The spinal nerve ligation model has been used commonly as a model for neuropathic pain (Kim and Chung, 1992; Tjølsen and Hole, 1997). We applied this model to the $Ca_v2.2$ mutant mice and quantified the extent of mechanical allodynia and thermal hyperalgesia accompanied by the neuropathic pain (Devor and Seltzer, 1999; Woolf and Mannion, 1999). The threshold for mechanical stimuli was determined by the von Frey test to assess mechanical allodynia, and the responses to heat stimuli were examined by the paw flick test to assess thermal hyperalgesia. As shown in Figure 6A and B, both $Ca_v2.2$+/+ and +/– mice developed robust mechanical allodynia and thermal hyperalgesia. On the other hand, $Ca_v2.2$–/– mice developed markedly reduced signs of neuropathic pain.

The N-type VDCC is known to be involved in the functions of the sympathetic nervous system, impairment of which might complicate the interpretation of the above-mentioned pain-related behaviors of the mutant mice. For example, impaired sympathetic function is thought to result in changes in body temperature, which might in turn affect paw withdrawal latency in the paw flick test. Therefore, we measured the peripheral body temperature of the mutant mice and compared it with that of wild-type

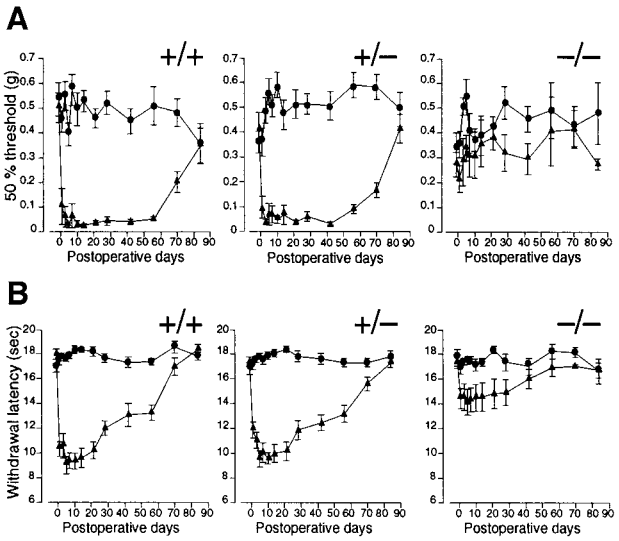

Fig. 6. Mechanical allodynia and thermal hyperalgesia induced by spinal nerve ligation. Fifty percent hindpaw withdrawal thresholds to stimulation with von Frey hairs (**A**) and hindpaw withdrawal latencies to thermal stimuli (**B**) are plotted against the days after the operation. Circles, uninjured side; triangles, operated side. +/+, wild-type; +/–, heterozygote; –/–, homozygous mutant. Homozygous mutants developed an attenuated post-operative decrease in the threshold and the latency, which are clearly observed in wild-type and heterozygous mutant mice as neuropathic pain symptoms. +/+, n = 9–13; +/–, n = 11–14; –/–, n = 5–8.

controls. However, the result shows no significant differences in the peripheral body temperature (29.0 ± 0.64°C for +/+, n = 8; 28.5 ± 0.37°C for +/–, n = 8; 28.2 ± 0.48°C for –/–, n = 5). We also examined the resting heart rate and blood pressure of the $Ca_v2.2$ mutant mice as indices for sympathetic nervous system functions, but again the data suggest no significant differences (heart rate: 564.3 ± 21.9 b.p.m. for +/+, n = 11; 617.7 ± 19.8 b.p.m. for +/–, n = 14; 547.0 ± 25.8 b.p.m. for –/–, n = 4; blood pressure: 107.3 ± 3.4/59.8 ± 2.6 mmHg for +/+, n = 11; 113.3 ± 2.6/64.5 ± 2.1 mmHg for +/–, n = 14; 111.6 ± 3.5/59.5 ± 2.8 mmHg for –/–, n = 4).

Discussion

In this study, we generated mice lacking the $\alpha_1 2.2$ subunit of the N-type VDCC. $Ca_v2.2$–/– mice showed a partial lethality, i.e. ~70% of the homozygous mutant mice survived to adulthood. This lethality is lower than that of mice lacking $Ca_v2.1$ (or homozygous for *leaner*, a hypomorphic allele for the *Cacna1a* gene encoding $Ca_v2.1$), which show almost fully penetrant lethality before weaning (Fletcher *et al*., 1996; Jun *et al*., 1999). The lower degree of lethality is also predicted by the results of studies with toxins that block VDCCs. Low doses of ω-agatoxins that block the $Ca_v2.1$ channel are lethal to rodents, but higher doses of ω-conotoxins that block the $Ca_v2.2$ channel are not (Chaplan *et al*., 1994b; Malmberg and Yaksh, 1994). However, the reason for the reduced viability in $Ca_v2.2$–/– mice is not clear and awaits further studies.

$Ca_v2.2$–/– mice displayed reduced anxiety-like behaviors, as assessed by the elevated plus-maze and open-field

tests, widely used tests to examine rodents' anxiety (Tarantino and Bucan, 2000). In addition, the results of the startle response tests are also consistent with the notion that the $Ca_v2.2$–/– mice have reduced anxiety. Although there remains a possibility that the reduced startle responses are due to an attenuated spinal reflex, this seems unlikely because locomotor activities were generally normal. The reduced level of anxiety in $Ca_v2.2$–/– mice is in contrast to the situation in the $Ca_v2.3$-null mice, which show rather enhanced anxiety-like behaviors (Saegusa *et al*., 2000). This suggests that the contribution of these channels to an animal's emotional state is different, although their expression domains in the brain overlap substantially (Williams *et al*., 1994; Ludwig *et al*., 1997). It may be interesting to dissect the molecular mechanisms that produced this difference in the emotional state in a future project.

$Ca_v2.2$–/– mice showed almost normal responses to acute nociceptive stimuli compared with $Ca_v2.2$+/+ mice, except for the responses in the tail flick test. It seems rather strange that $Ca_v2.2$–/– mice showed different responses in the two similar assays, paw flick and tail flick tests. The difference may be explained by the different sensitivities of the assays or by the possibility that different neural mechanisms underlie both assays. However, it is more conspicuous that $Ca_v2.2$–/– mice displayed some abnormal responses in the tests to quantify inflammatory pain. It is of interest that $Ca_v2.2$–/– mice showed a reduced level of responses only in the early half of phase 2 of the formalin test (Figure 5B). This early half of phase 2 seems to correspond to phase 2A reported by Yaksh and colleagues (Malmberg and Yaksh, 1992; Dirig *et al*., 1997). They proposed that phase 2 could be separated further into two qualitatively different subphases: phase 2A, the first half of phase 2 in which pain responses are sensitive to anti-inflammatory drugs such as cyclooxygenase inhibitors; and phase 2B, the latter half of phase 2 in which pain responses are resistant to these drugs (Malmberg and Yaksh, 1992; Dirig *et al*., 1997). Our result further confirmed the presence of two distinguishable subphases in phase 2 and indicates that phase 2A is completely dependent upon the N-type VDCC function. Previous studies using ω-conotoxins, however, showed that both phase 2A and phase 2B were dependent upon N-type VDCC function (Malmberg and Yaksh, 1994). This apparent discrepancy may be attributable to some compensation mechanisms that occurred only in phase 2B in the $Ca_v2.2$–/– mice. Elucidation of the exact mechanism by which the N-type channel controls the phase 2A responses awaits further studies, but one possibility is that the N-type VDCC controls release of neurotransmitters from the primary afferent fibers, which is induced by prostanoids generated by cyclooxygenases (White, 1996; Zimmer *et al*., 1998).

The $Ca_v2.2$–/– mice showed the increased level of phase 2 responses in the formalin test after sensitization with i.p. injection of acetic acid (Figure 5D), and in this case the phase 2A responses were also suppressed (data not shown). We previously reported that $Ca_v2.3$-null mice also showed reduced phase 2 responses in the normal formalin test and enhanced phase 2 responses after sensitization with a visceral noxious conditioning stimulus. In this respect, the effects of elimination of either the $Ca_v2.2$ or $Ca_v2.3$ channel seem to be similar. However, there was no differential effect on phase 2A and 2B in the case of $Ca_v2.3$-null mice, i.e. responses in both subphases were affected equally (unpublished observation). In this context, it is interesting that *Cacna1b* and *Cacna1e* (encoding the $Ca_v2.3$ channel) show different expression patterns in the RVM, where pain modulation mechanisms (both inhibitory and facilitatory) are thought to occur (Mason, 1999). Thus, both N- and R-type (coded by $Ca_v2.3$) VDCCs are involved in the inflammatory pain transmission and descending antinociceptive pathway, but the physiological roles of each channel seem to be quite different. Further studies are necessary to relate the expression of these channels and the abnormal phenotypes of the respective mutants.

Finally, and most importantly from a clinical point of view, the $Ca_v2.2$–/– mice showed a greatly reduced level of neuropathic pain symptoms. This unequivocally demonstrates that the N-type VDCC is essential for the mechanism to develop neuropathic pain, suggesting that blockers of this channel are useful for preventing neuropathic pain. However, it has been demonstrated that clinical application of ω-conopeptide has a limitation due to its side effects (Penn and Paice, 2000). Intrathecal injection of ω-conotoxin GVIA, the dose of which is enough to elicit motor deficits in $Ca_v2.2$+/+ mice, did not induce any overtly abnormal behaviors in $Ca_v2.2$–/– mice (our preliminary observation), suggesting that the side effects mentioned above result from the blockade of the N-type VDCC. Thus the fact that the $Ca_v2.2$–/– mice did not show any motor deficits might suggest some compensation mechanisms in $Ca_v2.2$–/– mice. Therefore, it may be important to explore the possible compensation mechanism in future studies. Otherwise, it would be difficult to use ω-conopeptides as antinociceptives avoiding their side effects.

Materials and methods

Gene targeting

Genomic clones containing the *Cacna1b* gene were screened from the 129/Sv mouse genomic library (Stratagene) with a 222 bp *Hin*dIII–*Hin*cII fragment (5′ linker–nucleotide 213) from pKCRB3 (Fujita *et al*., 1993) as a probe. Lambda phage clones were isolated and the inserts were subcloned into pBluescript II KS(+) (Stratagene).

Targeting vector BIIIZneoII was constructed using a 2.2 kb *Bgl*II–*Not*I fragment and a 6 kb *Xba*I–*Eco*RI fragment as 5′- and 3′-homologous regions, respectively (Figure 1A). A 1.6 kb region from the *Not*I site in exon 1 to an *Xba*I site in intron 1 was deleted, and *nlacZ* (a gene for *Escherichia coli* β-galactosidase with a nuclear localization signal at its N-terminus) was inserted in-frame. A positive selection marker (neomycin resistance gene driven by the phosphoglycerate kinase promoter) was also inserted in the direction opposite to that of *nlacZ* transcription. The diphtheria toxin A fragment gene driven by the MC1 promoter was used as a negative selection marker (Yagi *et al*., 1990).

BIIIZneoII was linearized with *Apa*I and electroporated into J1 ES cells (derived from the 129/Sv strain) (Li *et al*., 1992). Homologous recombinant ES cells were screened by Southern blot analysis. Mutant mice were generated by standard techniques (Papaioannou and Johnson, 1993). An F_1 heterozygous mutant with a hybrid background of C57Bl/6 (B6) and 129/Sv was backcrossed once against B6 and the resulting heterozygous offspring were intercrossed to obtain homozygous mutant mice.

Southern and northern blot analyses

Procedures are essentially the same as described (Saegusa *et al*., 2000). Probes were labeled with digoxigenin (DIG) using the DIG-High prime kit (Roche Molecular Biochemicals) and detected with alkaline

phosphatase (AP)-conjugated anti-DIG antibody. CSPD® or CDP-Star™ (Roche Molecular Biochemicals) was used as a substrate for AP.

RT–PCR

RT–PCR was essentially the same as reported (Saegusa *et al*., 2000). Primers used were mA1B-F1 (5′-ATGGTCCGCTTCGGGGAC-3′, corresponding to an upstream region from the *nlacZ* insertion site in exon 1 of *Cacna1b*) and mA1B-R1 (5′-AATGCAGTTGGCGATGATGG-3′, possibly located in exon 2). This primer pair yielded a 330 bp DNA fragment from normal *Cacna1b* cDNA.

Immunoblotting

The procedure is essentially the same as that reported previously (Saegusa *et al*., 2000) except that crude membrane fractions were prepared from hippocampi, because of the relatively abundant expression of the $Ca_v2.2$ channel in the hippocampus. The blot was probed with a rabbit polyclonal anti-$\alpha_1$2.2 (α_{1B}) or anti-$\alpha_1$2.3 (α_{1E}) antibody (both from Alomone Laboratories, Jerusalem, Israel).

Electrophysiological recording

DRG neurons from adult mice were acutely dissociated by a slight modification of the method of Scroggs and Fox (1992). Briefly, DRGs from the lower thoracic (T8) to lumbar level (L6) were quickly removed, treated with 2 mg/ml collagenase (type I, Sigma) and 2.5 mg/ml dispase I (Roche Molecular Biochemicals) in Tyrode solution (150 mM NaCl, 4 mM KCl, 2 mM $CaCl_2$, 2 mM $MgCl_2$, 10 mM HEPES and 10 mM glucose, adjusted to pH 7.4 with NaOH) at 37°C for 60 min, and then treated with dispase I alone at room temperature (22–25°C) for 60 min. DRG neurons were dissociated into single cells by trituration, plated on glass coverslips coated with poly-D-lysine (Sigma) and the coverslips were placed in a recording chamber on a microscope stage with superfusion (1.5 ml/min) with Tyrode solution.

Round-shaped DRG neurons were voltage-clamped by the conventional whole-cell patch–clamp techniques using an EPC-8 amplifier (HEKA, Germany) at room temperature (23–26°C). Pulse + Pulse Fit 8.11 software (HEKA) was used for data acquisition and analysis. In this study, we used relatively small DRG neurons (17–27 μm in diameter). These neurons would represent Aδ- and C-type DRG neurons, which are considered to transmit pain and thermal information under normal conditions (Raja *et al*., 1999). Patch pipets were pulled from thin-walled, fiber-filled borosilicate capillaries using a micropipet puller (Sutter Instrument, USA) and fire polished. Pipet resistance ranged from 4 to 8 MΩ when filled with the pipet solution described below. Gigaohm seal and entry into whole-cell mode were obtained in Tyrode solution. Series resistance was electronically compensated by 70–90%, and both the leakage and the remaining capacitance were corrected by the –P/4 method.

To isolate Ba^{2+} currents, the following solutions were employed: the pipet solution, 105 mM Cs-methanesulfonate, 4.5 mM $MgCl_2$, 10 mM EGTA, 10 mM HEPES–CsOH, 4 mM Na_2ATP, 1 mM NaGTP and 15 mM creatine phosphate, adjusted to pH 7.3 with CsOH (293 mOsM); the external solution, 160 mM tetraethylammonium chloride, 2 mM $BaCl_2$, 10 mM HEPES–CsOH, 10 mM glucose, 0.001 mM tetrodotoxin, adjusted to pH 7.4 with CsOH (310 mOsM). Data were filtered at 3–5 kHz (four-pole Bessel filter) and sampled at 5 kHz. In the experiments with ω-conotoxin GVIA and ω-agatoxin IVA (Peptide Institute, Inc., Osaka, Japan), the external solution was supplemented with 0.1 mg/ml cytochrome *c*. The blocking effects of these toxins on Ba^{2+} current amplitude were estimated from the plots of peak current versus time, with run-down taken into account as described previously (Scroggs and Fox, 1991). All data are presented as mean ± SEM, and statistical significance was assessed by Mann–Whitney test.

Behavioral studies

All the experiments were conducted under the ethical guidelines for the study of experimental pain in conscious animals (International Association for the Study of Pain, 1995), and the protocol of the pain behavioral studies described here has been approved by the Animal Care Committee of Tokyo Medical and Dental University. All the experiments were performed in a blind manner. The data were expressed as mean ± SEM and analyzed by Tukey test for multiple comparisons or by Student's *t*-test for comparison between groups. Open-field, elevated plus-maze, startle response, von Frey, paw flick, tail flick, hot plate, formalin and acetic acid writhing tests were carried out according to the methods described previously (Saegusa *et al*., 2000).

Tail pressure test. The local pressure required to elicit tail withdrawal was quantified with an Ugo Basile Analgesymeter (Ugo Basile, Italy). The nociceptive threshold was defined as the force in grams.

Neuropathic pain model. Spinal nerve ligation was carried out under sodium pentobarbital anesthesia as described previously (Kim and Chung, 1992). Briefly, a midline incision was made in the skin of the back at the L4–S2 levels and the right paraspinal muscles were separated from the spinous processes, facet joints and transverse processes at the L4–S1 levels. The L5–L6 transverse processes were removed, and the right L5 and L6 spinal nerves were ligated tightly with 8-0 silk thread.

Acknowledgements

We thank M.Kondoh, M.Tamura, E.Tominaga, T.Muno, N.Yoneda, S.Inada, L.Gunsten, C.Le and staff at Animal Research Center of Tokyo Medical and Dental University for assistance, Professor T.Noda for kindly providing us with the cloning vectors for gene targeting and J1 ES cells, Drs M.Osanai and Y.Sakata for technical advice, and Dr T.Murakoshi for critically reading the manuscript. This work was supported by grants from the Ministry of Health and Welfare, the Ministry of Education, Science, Sports and Culture, Japan, the Uehara Memorial Foundation and the Naito Memorial Foundation.

References

Bowersox,S.S., Gadbois,T., Singh,T., Pettus,M., Wang,Y.-X. and Luther,R.R. (1996) Selective N-type neuronal voltage-sensitive calcium channel blocker, SNX-111, produces spinal antinociception in rat models of acute, persistent and neuropathic pain. *J. Pharmacol. Exp. Ther.*, **279**, 1243–1249.

Catterall,W.A. (1998) Structure and function of neuronal Ca^{2+} channels and their role in neurotransmitter release. *Cell Calcium*, **24**, 307–323.

Chaplan,S.R., Bach,F.W., Pogrel,J.W., Chung,J.M. and Yaksh,T.L. (1994a) Quantitative assessment of tactile allodynia in the rat paw. *J. Neurosci. Methods*, **53**, 55–63.

Chaplan,S.R., Pogrel,J.W. and Yaksh,T.L. (1994b) Role of voltage-dependent calcium channel subtypes in experimental tactile allodynia. *J. Pharmacol. Exp. Ther.*, **269**, 1117–1123.

Chapman,C.R., Casey,K.L., Dubner,R., Foley,K.M., Gracely,R.H. and Reading,A.E. (1985) Pain measurement: an overview. *Pain*, **22**, 1–31.

Devor,M. and Seltzer,Z. (1999) Pathophysiology of damaged nerves in relation to chronic pain. In Wall,P.D. and Melzack,R. (eds), *Textbook of Pain*. Churchill Livingstone, London, pp. 129–164.

Diaz,A. and Dickenson,A.H. (1997) Blockade of spinal N- and P-type, but not L-type, calcium channels inhibits the excitability of rat dorsal horn neurones produced by subcutaneous formalin inflammation. *Pain*, **69**, 93–100.

Dirig,D.M., Konin,G.P., Isakson,P.C. and Yaksh,T.L. (1997) Effect of spinal cyclooxygenase inhibitors in rat using the formalin test and *in vitro* prostaglandin E_2 release. *Eur. J. Pharmacol.*, **331**, 155–160.

Ertel,E.A. *et al*. (2000) Nomenclature of voltage-gated calcium channels. *Neuron*, **25**, 533–535.

Fletcher,C.F., Lutz,C.M., O'Sullivan,T.N., Shaughnessy,J.D.,Jr, Hawkes,R., Frankel,W.N., Copeland,N.G. and Jenkins,N.A. (1996) Absence epilepsy in tottering mutant mice is associated with calcium channel defects. *Cell*, **87**, 607–617.

Fujita,Y. *et al*. (1993) Primary structure and functional expression of the ω-conotoxin-sensitive N-type calcium channel from rabbit brain. *Neuron*, **10**, 585–598.

Hofmann,F., Lacinova,L. and Klugbauer,N. (1999) Voltage-dependent calcium channel: from structure to function. *Rev. Physiol. Biochem. Pharmacol.*, **139**, 33–87.

International Association for the Study of Pain (1995) In Fields,H.L. (ed.), *Core Curriculum for Professional Education in Pain.* IASP, Seattle, WA, pp. 111–112.

Jun,K. *et al*. (1999) Ablation of P/Q-type Ca^{2+} channel currents, altered synaptic transmission and progressive ataxia in mice lacking the α_{1A}-subunit. *Proc. Natl Acad. Sci. USA*, **96**, 15245–15250.

Kim,S.H. and Chung,J.M. (1992) An experimental model for peripheral neuropathy produced by segmental spinal nerve ligation in the rat. *Pain*, **50**, 355–363.

Kurihara,T., Nonaka,T. and Tanabe,T. (2000) A noxious visceral conditioning stimulus evokes long-lasting inhibition of somatic inflammatory pain. *Jpn J. Pharmacol.*, **82**, Suppl. 1, 163 (abstract).

Li,E., Bestor,T.H. and Jaenisch,R. (1992) Targeted mutation of the DNA

methyltransferase gene results in embryonic lethality. *Cell*, **69**, 915–926.

Ludwig,A., Flockerzi,V. and Hofmann,F. (1997) Regional expression and cellular localization of the α_1 and β subunit of high voltage-activated calcium channels in rat brain. *J. Neurosci.*, **17**, 1339–1349.

Malmberg,A.B. and Yaksh,T.L. (1992) Antinociceptive actions of spinal nonsteroidal anti-inflammatory agents on the formalin test in rats. *J. Pharmacol. Exp. Ther.*, **263**, 136–146.

Malmberg,A.B. and Yaksh,T.L. (1994) Voltage-sensitive calcium channels in spinal nociceptive processing: blockade of N- and P-type channels inhibits formalin-induced nociception. *J. Neurosci.*, **14**, 4882–4890.

Mason,P. (1999) Central mechanisms of pain modulation. *Curr. Opin. Neurobiol.*, **9**, 436–441.

Neugebauer,V., Vanegas,H., Nebe,J., Rümenapp,P. and Schaible,H.-G. (1996) Effects of N- and L-type calcium channel antagonists on the responses of nociceptive spinal cord neurons to mechanical stimulation of the normal and the inflamed knee joint. *J. Neurophysiol.*, **76**, 3740–3749.

Papaioannou,V. and Johnson,R. (1993) Production of chimeras and genetically defined offspring from targeted ES cells. In Joyner,A.L. (ed.), *Gene Targeting: A Practical Approach*. IRL Press, Oxford, pp. 107–146.

Penn,R. and Paice,J.A. (2000) Adverse effects associated with the intrathecal administration of ziconotide. *Pain*, **85**, 291–296.

Piedras-Renteria,E.S. and Tsien,R.W. (1998) Antisense oligonucleotides against α_{1E} reduce R-type calcium currents in cerebellar granule cells. *Proc. Natl Acad. Sci. USA*, **95**, 7760–7765.

Raja,S.N., Meyer,R.A., Ringkamp,M. and Campbell,J.N. (1999) Peripheral neural mechanism of nociception. In Wall,P.D. and Melzack,P. (eds), *Textbook of Pain*. Churchill Livingstone, London, pp. 11–57.

Sabath,D.E., Broome,H.E. and Prystowsky,M.B. (1990) Glyceraldehyde-3-phosphate dehydrogenase mRNA is a major interleukin 2-induced transcript in a cloned T-helper lymphocyte. *Gene*, **91**, 185–191.

Saegusa,H. *et al*. (2000) Altered pain responses in mice lacking α_{1E} subunit of the voltage-dependent Ca^{2+} channel. *Proc. Natl Acad. Sci. USA*, **97**, 6132–6137.

Scroggs,R.S. and Fox,A.P. (1991) Distribution of dihydropyridine and ω-conotoxin-sensitive calcium current in acutely isolated rat and frog sensory neuron somata: diameter-dependent L channel expression in frog. *J. Neurosci.*, **11**, 1334–1346.

Scroggs,R.S. and Fox,A.P. (1992) Calcium current variation between acutely isolated adult rat dorsal root ganglion neurons of different size. *J. Physiol. (Lond.)*, **445**, 639–658.

Sluka,K.A. (1998) Blockade of N- and P/Q-type calcium channels reduces the secondary heat hyperalgesia induced by acute inflammation. *J. Pharmacol. Exp. Ther.*, **287**, 232–237.

Tarantino,L.M. and Bucan,M. (2000) Dissection of behavior and psychiatric disorders using the mouse as a model. *Hum. Mol. Genet.*, **9**, 953–965.

Tjølsen,T. and Hole,K. (1997) Animal models of analgesia. In Dickenson,A. and Besson,J.-M. (eds), *The Pharmacology of Pain*. Springer-Verlag, Berlin, pp. 1–20.

Tottene,A., Volsen,S. and Pietrobon,D. (2000) α_{1E} subunits form the pore of three cerebellar R-type calcium channels with different pharmacological and permeation properties. *J. Neurosci.*, **20**, 171–178.

Vanegas,H. and Schaible,H.-G. (2000) Effects of antagonists to high-threshold calcium channels upon spinal mechanism of pain, hyperalgesia and allodynia. *Pain*, **85**, 9–18.

White,D.M. (1996) Mechanism of prostaglandin E_2-induced substance P release from cultured sensory neurons. *Neuroscience*, **70**, 561–565.

Williams,M.E. *et al*. (1994) Structure and functional characterization of neuronal α_{1E} calcium channel subtypes. *J. Biol. Chem.*, **269**, 22347–22357.

Witcher,D.R., De Waard,M., Sakamoto,J., Franzini-Armstrong,C., Pragnell,M., Kahl,S.D. and Campbell,K.P. (1993) Subunit identification and reconstitution of the N-type Ca^{2+} channel complex purified from brain. *Science*, **261**, 486–489.

Woolf,C.J. and Mannion,R.J. (1999) Neuropathic pain: aetiology, symptoms, mechanism and management. *Lancet*, **353**, 1959–1964.

Yagi,T., Ikawa,Y., Yoshida,K., Shigetani,Y., Takeda,N., Mabuchi,I., Yamamoto,T. and Aizawa,S. (1990) Homologous recombination at c-*fyn* locus of mouse embryonic stem cells with use of diphtheria toxin A-fragment gene in negative selection. *Proc. Natl Acad. Sci. USA*, **87**, 9918–9922.

Zhang,J.F., Randall,A.D., Ellinor,P.T., Horne,W.A., Sather,W.A., Tanabe,T., Schwarz,T.L. and Tsien,R.W. (1993) Distinctive pharmacology and kinetics of cloned neuronal Ca^{2+} channels and their possible counterparts in mammalian CNS neurons. *Neuropharmacology*, **32**, 1075–1088.

Zimmer,A., Zimmer,A.M., Baffi,J., Usdin,T., Reynolds,K., Koenig,M., Palkovits,M. and Mezey,E. (1998) Hypoalgesia in mice with a targeted deletion of tachykinin 1 gene. *Proc. Natl Acad. Sci. USA*, **95**, 2630–2635.

Received November 20, 2000; revised March 15, 2001; accepted March 19, 2001